doi: 10.1111/j.1460-2695.2004.00830.x

The relationship between process mechanisms and crack paths in friction stir welded 5083-H321 and 5383-H321 aluminium alloys

M. N. JAMES[1], G. R. BRADLEY[2], H. LOMBARD[3] and D. G. HATTINGH[3]

[1]*Faculty of Technology, University of Plymouth, Plymouth PL4 8AA, UK,* [2]*Department of Mechanical Engineering, University of Sheffield, Sheffield S1 3JD, UK,* [3]*Department of Mechanical Engineering, PE Technikon, Private Bag X6011, Port Elizabeth 6001, South Africa*

Received in final form 31 March 2004

ABSTRACT Friction stir (FS) welding is a relatively new solid-state welding process that offers high levels of joint performance with minimal preparation and little post-weld dressing. The high levels of plastic work induced in the weld zone produce a very fine grain size in the stirred region of the weld (e.g. the nugget), while the low heat input limits residual stresses to a low fraction of the proof strength of the weld metal. These effects are generally beneficial to weld dynamic performance. The peculiar thermomechanical history in the FS weld region leads, however, to particular defects with some unusual effects on crack path, whose occurrence depends partly on crack speed, or growth rate. This paper presents observations regarding specific influences of the FS welding process on crack paths and dynamic performance for 5083-H321 and 5383-H321 aluminium alloys, and proposes an explanation for the observations in terms of the weld microstructures and thermomechanical history. The insights presented in this paper can be used to inform optimisation of the weld process parameters, through on-line feedback and control of tool geometry, force footprint, torque and temperature.

Keywords fatigue performance; force footprint; friction stir welding; strain partitioning; weld defects.

INTRODUCTION

Crack paths in fatigue and fracture are complex and difficult to predict, despite a significant body of knowledge regarding the mechanics of crack growth. The field of fracture mechanics, which deals with the behaviour of cracked bodies under load, is now widely regarded as 'mature', in the sense that solutions exist to describe the conditions for crack growth and the path that an ideal crack would take.[1] In practice, however, real materials and microstructures are not homogeneous or isotropic, nor are they *continua* in the manner usually assumed by mechanics descriptions.

Thus microstructure and mechanical property variation can interact in relatively subtle ways with fluctuations in applied load and environment. The net result of these interactions is a complexity to crack paths that is incompletely understood at the present time, even under straightforward cases of uniaxial loading. The research community in fatigue crack growth has been exposed for long enough to this complexity, that general assumptions of similarity in origin are often imposed in the interpretation of features of crack paths that arise from new processes or materials. When this is done, it is important to ensure that proposed mechanisms encompass all the relevant aspects of the process–structure–property interaction. Although fractography has revealed much about the microscopic mechanisms of fatigue, it is most useful as a tool to provide supporting evidence for theories developed from other considerations. Interpretation of fracture surface features, in the absence of full information regarding their possible causes, is known to be fraught with uncertainty.

The present paper will illustrate this complexity in relation to identifying subtleties in crack path mechanisms for the case of friction stir (FS) welded 5083-H321 and 5383-H321 aluminium alloys. FS welding is a relatively new solid-state process that involves plunging a rotating tool into the joint between faying plates. Once the weld zone has reached an appropriate thermo-mechanical state, the tool is traversed along the joint line and the weld is made by pick-up and transfer of material around the tool, to be then deposited behind it. Figure 1 illustrates the main features associated with a single-pass (SP) FS welded joint.

Correspondence: M. N. James. E-mail: mjames@plymouth.ac.uk

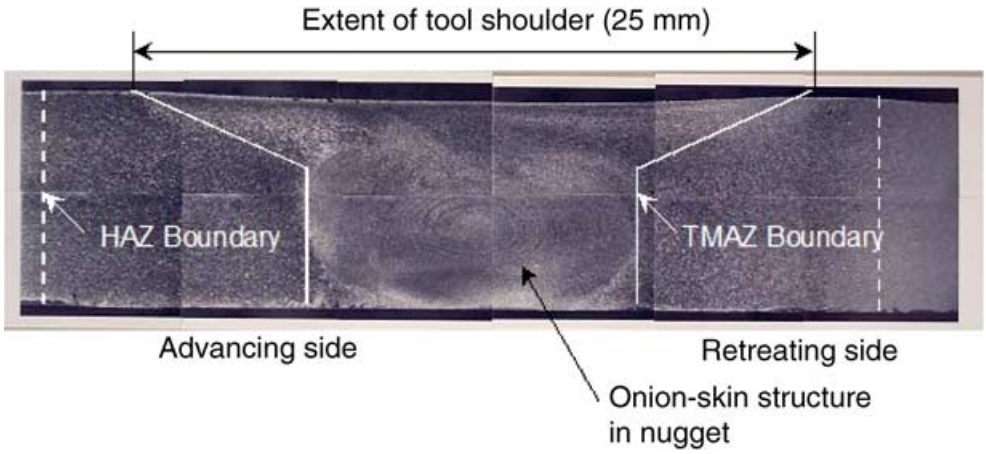

Fig. 1 Illustration of the main features associated with a macro-etched SP FS weld.

Currently, appropriate process conditions to make a 'sound' FS weld are determined empirically, and it is not easy to obtain values for the energy input into unit length of the weld.

The advancing side of the weld is defined as existing where the translational velocity along the weld line is additive with the rotational velocity of the tool. The retreating side is the opposite, and the rotational velocity is hence subtractive from the translation. The extensive mechanical work put into the thermomechanically affected weld zone (TMAZ) leads to a fine-grained structure in the weld nugget, which often etches up as an 'onionskin' structure both in cross section and along the length of the weld.

It might be expected that this structure would be reflected in crack paths and, as will be detailed in this paper, this does occur to a certain extent. The more interesting aspects relate to the subtlety of the underlying mechanism through which the structure/path interaction is evidenced in, at least, certain FS welded alloys, and the ways in which this affects fatigue and fracture performance. The fractographic evidence offers little insight into the mechanism of the structure/path interaction and can be readily interpreted in a misleading way.

To illustrate this, consider the fracture surface shown in Fig. 2. The fracture surface shows a fatigue crack at the right of the figure, with fast fracture to the left of the fatigue region. A large planar facet, some 1.5 mm in length (marked with the arrows), can be seen in the fast fracture region. Such apparent defect indications are of significant concern, as a major advantage of the FSW process is the absence of cast material in the weld zone and an associated reduction in potential defect population.

Considering the nature of the FSW deformation processes, which involve material entrainment around the tool and subsequent deposition in its wake under the forging action of the tool shoulder, this apparent indication of a defect seems likely to reflect some aspect of the necessary deformation and forging processes. Indeed, such an explanation was proposed when these features were first observed by the present authors[2] and they were then referred to as 'partial-forging defects'. Subsequent work has led to a refinement of ideas regarding their formation, the conclusions of which are supported by related work from other researchers.

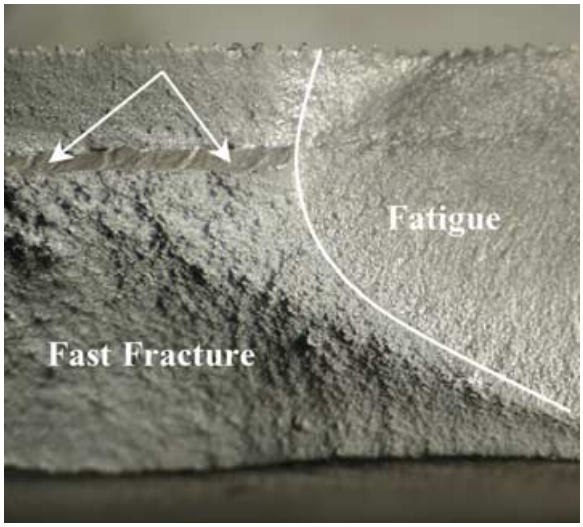

Fig. 2 Optical fractograph of an 8 mm thick SP FSW fatigue specimen.

Thus the intention in this paper is to discuss potential FSW defects in general terms, and then to address specific fractographic defect 'indications' for FS welded fatigue specimens in 5383-H321 and 5083-H321 aluminium alloys. It will examine the role of process–structure interactions both in generating such defect indications, and in influencing crack paths, and will consider the effect of these planar defects on dynamic performance of the welds.

This leads to some general conclusions as to the manner in which FSW process parameters might be optimised so as to minimize any detrimental influence on fatigue and fracture. This paper presents initial findings in this respect using force 'footprint' data obtained from an instrumented FSW tool using on-line control of welding travel speed and tool rotational speed.

DEFECTS IN FS WELDS

As stated above, defect levels are generally low in FSW, compared with typical fusion welds. A number of types of defect are known to occur, however, and because they can occur in any orientation and at any angle, may be difficult to detect with directionally specific techniques such as radiography and ultrasonics.[3] The known defects in FS butt welds include lack of penetration (tool length too small for the plate thickness), voids and root defects, which are also known as 'kissing bonds.' Tool penetration is generally around 90% of the plate thickness, and can therefore lead to defective welds if, for example, plate thickness is variable along the weld line. This is essentially a process-control problem that can be resolved by appropriate seam-tracking devices, e.g. downward force on the tool.

Voids

Voids have been proposed to occur as consequence of the fluid dynamics associated with the plastic flow in the weld zone.[4] Numerical three-dimensional modelling of the flow dynamics in the weld region has indicated that there is a zone on the advancing side of the weld where chaotic flow occurs. It has been proposed that there is a location within this zone above and below which the flow is in opposite directions, creating a vortex.[4] Such vortices could lead to the generation of a series of voids in the weld zone, potentially with significant sizes. Voids do occur in FS welds, and sometimes can be seen on the surface of fatigue specimens machined from welded plates, i.e. that occurred in the interior of the original weld. Figure 3 shows such voids observed metallographically on the surface of a reversed bend fatigue specimen. The largest void is some 368 μm by 279 μm and, under certain conditions, such large defects would be expected to have a very significant effect on crack initiation and/or crack paths and hence on fatigue life.

Figure 4a provides supporting evidence for this influence on fatigue life and shows the crack initiation region on the fracture surface for the specimen containing the voids seen in Fig. 3. This specimen was tested at a peak surface stress of 196 MPa and returned a life of 50 723 cycles, a much lower value than those pertaining to specimens tested at stresses at either side of 196 MPa (see Table 1). Table 1

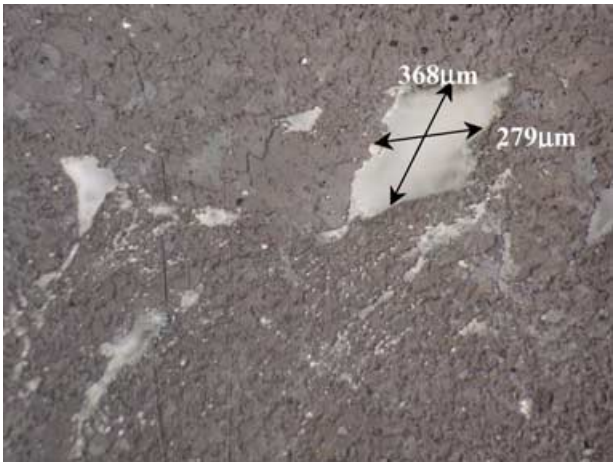

Fig. 3 Large void observed in the welded region on an FSW fatigue specimen.

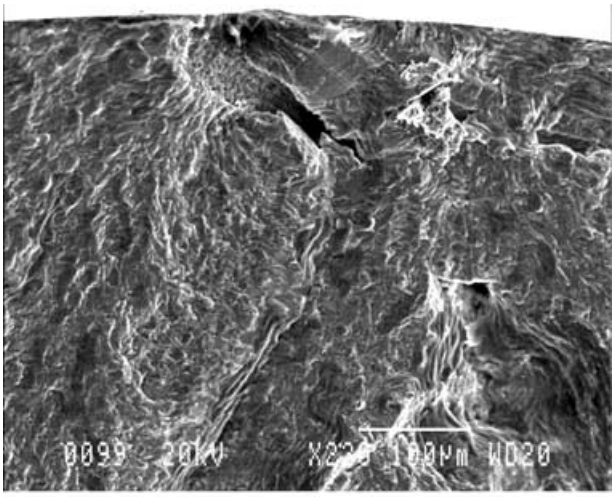

Fig. 4 (a) Void assisted crack initiation in SP FSW reversed bend fatigue specimen. (b) Fractographic evidence of dynamic recrystallisation in FSW.

Table 1 Fatigue life for 6 mm diameter reversed bend FSW specimens

Stress amplitude (MPa)	Cycle life N_f	Failure distance from weld centreline (mm)
261	15 873	5.5
240	36 332	5.5
213	192 167	0.5
196	50 723	2.5
176	185 000	4.5
173	673 509	6
169	299 784	0
136	285 024	1.5
130	1 204 153	3.5

gives S–N data obtained under reversed bending from polished hourglass specimens with the weld zone centrally positioned in the gauge length. Void assisted crack initiation has also been observed by the present authors at the surface of full-plate-depth fatigue specimens, and it therefore seems likely that voiding can occur at all depths in FSW joints.

This then leads to doubts that all voids arise from fluid dynamic processes. There is still argument in the FSW research community regarding the kinetics and dynamics of the process, and fractographic information may assist in interpretation of the underlying mechanisms. Equally, a thorough understanding of the process-microstructure-performance characteristics of FS welds will contribute to crack path analysis and can contribute to eventual process-performance optimisation. As an example of this, which is related to the mechanisms of void formation, consider the magnified view of the crack initiation region in Fig. 4a, which is given as Fig. 4b.

Dynamic recrystallisation is still a topic of controversy amongst FSW researchers, although substantial evidence exists for continuous dynamic recrystallisation in FSW of aluminium alloys.[5] Figure 4b shows clear evidence of dynamic recrystallisation in the fine (10 μm average diameter) polygonal grains, which are marked with arrow A. Grain growth is indicated in the variety of grain sizes present. Interestingly, this mechanism of grain formation is shown up because some of these regions (arrows labelled A and B) represent crack path defects and are here associated with voids in the material. The polygonal shape of the voids seen in Fig. 3 raises the question of their provenance. Voids associated with a vortex generation mechanism would be expected to be circular or elliptical in shape, and such voids are sometimes found on the fracture surfaces of FSW specimens (Fig. 5). In contrast, it can be speculated that the voids seen in Fig. 3 have their origin and/or shape linked in some way to the occurrence of dynamic recrystallisation, rather than vortex shedding.

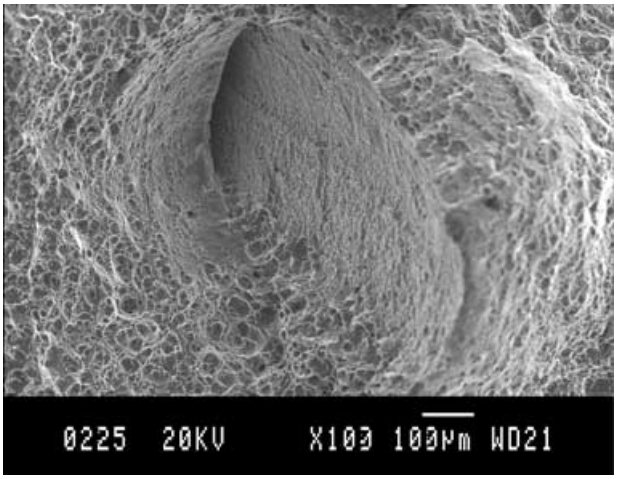

Fig. 5 Elliptical void on the fracture surface of an FSW specimen.

The discussion thus far does not make clear why regions such as the one indicated with the arrow marked A, apparently form weak interfaces in the TMAZ of the weld. A hypothesis is advanced later in the paper regarding strain localisation effects in the onionskin structure that may, however, offer an explanation of some of the features associated with crack paths in both figures, i.e. Figs 2 and 4b.

Root defects

Root defects or 'kissing bonds' occur when the root of a single pass weld achieves only partial bonding and their effect on fatigue strength is covered in a paper by Dickerson and Pryzdatek.[6] The occurrence of kissing bonds appears to be alloy specific and in particular, in the limited range of alloys considered, 5038-H321 is known to be more susceptible to these defects than either 5083-O or 6082-T6 alloys.[6] They are difficult to detect using either radiography or dye penetrant techniques[6] but can have an effect on fatigue performance if the root flaw is >0.35 mm in depth.

The relative difficulty of detecting defects in FS welds makes it imperative to fully understand their influence on fatigue crack initiation and total life. It would also be advantageous to know their dependence on process parameters, such as tool travel speed, rotational speed and geometry. As yet, however, there is an absence of detailed information particularly regarding internal defects, their mechanism of origin and influence on fatigue crack initiation and life. The few reported studies in this area are often preliminary in nature, which cover only limited ranges of controlling parameters.[6,7] These studies have tended to find minimal effect of defects on the fatigue performance of FSW joints, but work by the present authors has indicated more serious consequences both of voids and of

crack path defects associated with the onionskin structure. These aspects will be considered in the following sections.

INFLUENCE OF FSW DEFECTS ON CRACK PATHS AND FATIGUE PERFORMANCE

Material and experimental conditions

The work reported in this paper was carried out on fatigue specimens machined from FSW butt joints made between 8 mm thick plates of 5083-H321 or 5383-H321 aluminium alloys. All welds were made at TWI under empirically determined conditions that gave sound welds, at least as judged by the absence of root defects and any significant radiographic defect indications. These conditions can be summarized as using a Type 5651 tool (25 mm shoulder, pin diameter of 10 mm and a length of 7.9 mm) using a tool rotational speed of 500 rpm clockwise, looking at the plate, a forward tool tilt in the direction of travel of 2.5° and a heel plunge depth of 0.2 mm. Weld travel speed was kept constant for a particular weld, but varied between 60 mm/min and 200 mm/min. This variation in weld pitch (defined here as travel speed over tool rotational speed) from 0.12 mm/rev to 0.40 mm/rev, had the aim of examining whether certain crack path defects associated with the onionskin structure increased in frequency as travel speed increased for a set tool rotational speed. This is equivalent to a decrease in energy input per unit length of weld, on the assumption that tool speed and feed are the major sources of energy input into the weld metal. In the event, no systematic variation in defect occurrence was noticed over this range of weld pitch values and welds made under these conditions appear to be comparable in fatigue terms. The chemical composition and mechanical property data for the two alloys are given in Table 2.

Friction stir welding reduces the 0.2% proof strength of the alloy from the parent plate value of around 264–275 MPa to about 160 MPa in the weld TMAZ region. Vickers hardness values (HVN) under a 200 gf load drop from around 105 in the parent plate to 81–85 within the TMAZ, which extends out to about 15 mm on either side of the weld centreline. These hardness values are little affected by the present range of weld process conditions, as indicated in Fig. 6 for 5383-H321 plate welded at 80 mm min^{-1} and for 5083-H321 welded at 200 mm min^{-1}. This observation supports that of the lack of any systematic effect of these process conditions on fatigue performance. The mean hardness value in the weld metal with the faster travel speed is approximately 90 Vickers, while that for the 80 mm min^{-1} travel speed is around 87.5 Vickers. This difference is less than local variations in hardness values that can be seen in the weld zone, averaging around 5 HVN, with occasional spikes >10 HVN. It is possible that this is related to the existence of the onionskin structure in the weld TMAZ, in line with the discussion given later in the paper, and further work on interpreting TMAZ microstructures is in progress.

Several different types of fatigue load and specimen have been considered in this work. That part primarily dealing with travel speed effects used rectangular section, hourglass-shaped fatigue specimens. Gauge length of the specimens was 40 mm, width 16 mm and thickness was kept as close as possible to the original plate size of approximately 8 mm. A 100 mm radius was used to connect the gauge length to the grip sections, and the edges were slightly rounded to prevent crack initiation occurring there. S–N testing was performed in tension at 112 Hz and $R = -1$ (fully reversed loading). Two specimen surface conditions were used: (1) as-welded, with small burrs at the edges of the weld region removed, but the tool shoulder ledges (~0.2 mm) remaining, and (2) machined, where both burrs and ledges had been removed, leaving a smooth surface free of stress concentrations (net thickness about 7.4 mm). This was done because there was interest in both the fatigue performance of as-welded samples, representing general engineering usage, and in the inherent fatigue properties of the welds as a function of travel speed, unaffected by surface artefacts induced by the welding process.

Further work on the influence of defects on crack paths was performed using 6 mm diameter hourglass specimens tested at $R = -1$ in reversed bend. These specimens had a polished surface and therefore also bypass crack initiation from artefacts of the welding process (i.e. ledges at weld edge and tool travel marks). The gauge section in these specimens was only 8 mm and the weld and specimen centrelines were arranged to coincide. This confined crack initiation largely to the weld nugget region.

Table 2 Chemical composition and mechanical property data

Weight%	Mg	Mn	Si	Fe	Cr	Zn	Cu	Ti	$\sigma_{0.2\%}$ (MPa)	σ_{TS} (MPa)
5083-H321	4.20	0.60	0.25	0.15	0.09	0.09	0.06	0.02	264	350
5383-H321	4.75	0.82	0.11	0.12	0.08	0.22	0.08	0.03	275	370

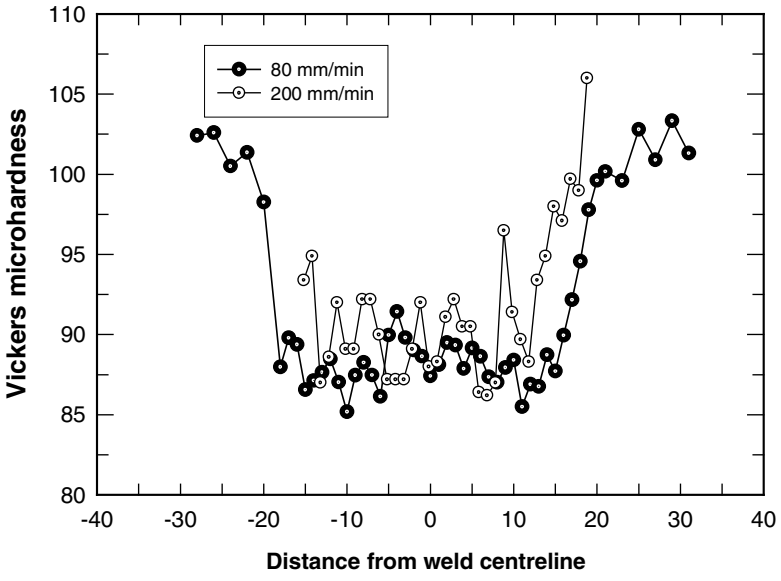

Fig. 6 Microhardness variation across typical FSW joints in 5×83-H321 aluminium alloy.

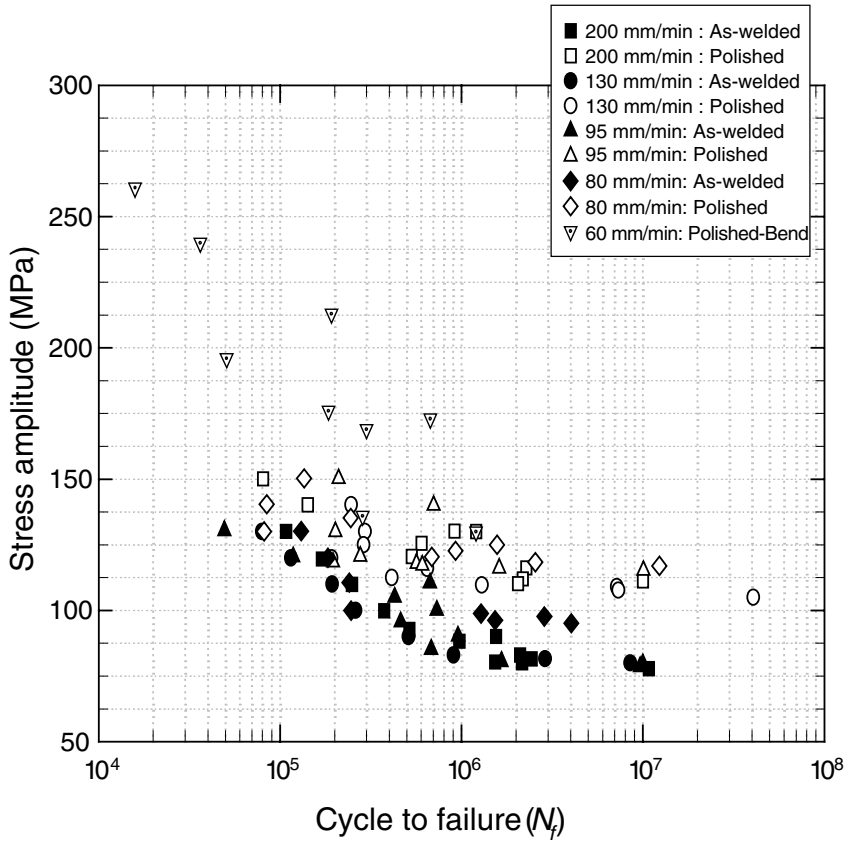

Fig. 7 S–N data for reversed tension and bend fatigue in SP FSW specimens of 5×83-H321 aluminuim alloy.

Fatigue performance

The reversed bend fatigue data given in Table 1 are plotted in Fig. 7, together with data obtained from the tension tests. It is immediately clear from the figure that the smaller polished bend specimens generally show much higher fatigue strengths than the larger tension specimens. Tension tests are known to give lower fatigue strengths than equivalent bend tests, because the whole cross-sectional area experiences peak stresses in the

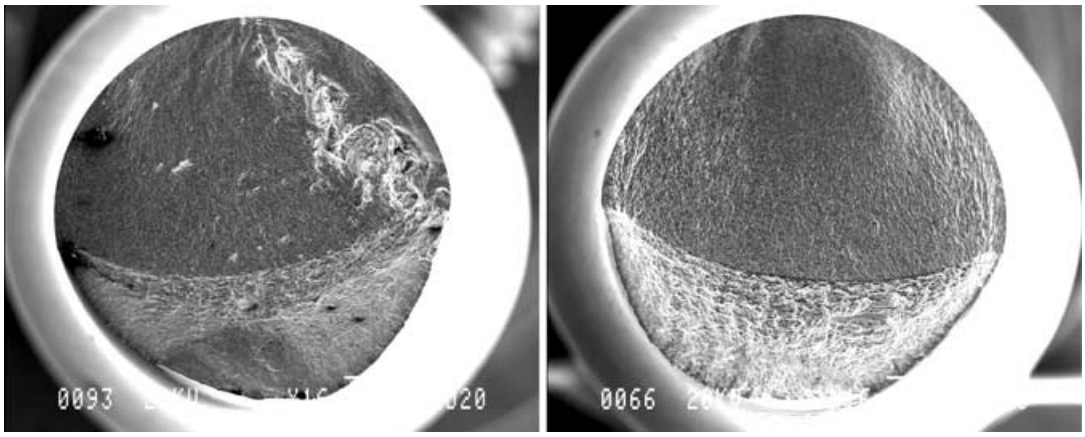

Fig. 8 Low-magnification fractographs of reversed bend fatigue specimens with (a) (LHS) defect-influenced crack initiation and growth and (b) (RHS) initiation uninfluenced by defects.

fatigue loading. The difference would not be expected to be this marked, however, and these data are therefore likely to reflect defect influences in the larger cross section of the tension specimens (128 mm^2 compared with 28 mm^2 for the bend specimens). In support of this argument, the poorer performing bend specimens, where large defects influenced crack initiation, fall into the same scatter band as the polished tension specimens (tension data at stress amplitudes of 196, 136 and 130 MPa).

Figure 8 compares typical low-magnification fractographs for reversed bend specimens in cases where defects have influenced crack initiation and crack paths, as well as where they have not had such a role. The defects shown in Fig. 8a (left-hand side of the picture with $N_f =$ 50 732 cycles at $\sigma_{amplitude} = 196$ MPa) have reduced the fatigue performance of the specimen by a factor of around 2.6 on life (equivalent to a reduction in fatigue strength of about 15%), compared with that of the specimen shown in Fig. 8b (right-hand side of the picture with $N_f = 185\,000$ cycles at $\sigma_{amplitude} = 176$ MPa).

Similar observations can be drawn regarding the tension specimens. Close analysis of the fatigue data at various travel speeds[2] demonstrated both that defects could influence fatigue performance in these specimens, and that the onionskin TMAZ structure manifested itself in at least two different effects on the crack path, namely large planar facets and banding on the fracture surface. The banding is very likely to be related to the recrystallization structure shown in Fig. 4b. Such observations allow some useful conclusions to be drawn in the next section, regarding the origin of, and mechanism behind, the planar regions seen on the fracture surfaces of FSW specimens. In addition, polygonal voids did occur and were occasionally observed influencing crack initiation.

The combined effects of voids and planar facets (which provide, e.g. easy fracture paths linking two small fatigue cracks) led to reductions in fatigue strength of around 15–20%, compared with specimens where such defects did not occur. These observations indicate that the issue of defects in FS welds, their origins and alloy dependence, and their effects on initiation and crack paths would clearly benefit from further attention by the research community.

Crack path defects

FSW crack path defects in 5083-H321 and 5383-H321 include the flat regions seen in Fig. 4b, which reflect details of the recrystallized grain structure and are probably related to banding observed on other fracture surfaces (see Fig. 9a). They also include much larger planar facets on the fracture surface (Figs 9b and c), which occur more frequently when the crack growth rates are higher and when the cracks are larger.[2] These represent crack growth conditions where crack tip plastic zones are larger, and the strain rates in the plastic zones are higher. The defects are particularly prevalent in the fast fracture region.

It seems reasonable that crack path defect behaviours in FS welds that are triggered by crack plasticity effects, reflect the mechanisms of thermo-mechanical deformation that led to the onionskin structure observed in the TMAZ region. As not all FS welds show such a structure in the TMAZ, proving this linkage would be of benefit in identifying process-optimization routes to minimize the thermo-mechanically induced layered structure and its effects on dynamic performance.

The results summarized in this paper, and those reported in Ref. [2], therefore led to the proposal that a particular class of planar crack path defects in FSW arise from the plastic flow processes involved in generating the layers in the onionskin structure. As seen in Fig. 9b, the large planar facets can occur in sequences reflecting the tool pitch, around 0.16 mm in the case shown, and hence they are likely to be associated with layer interfaces. While the de-

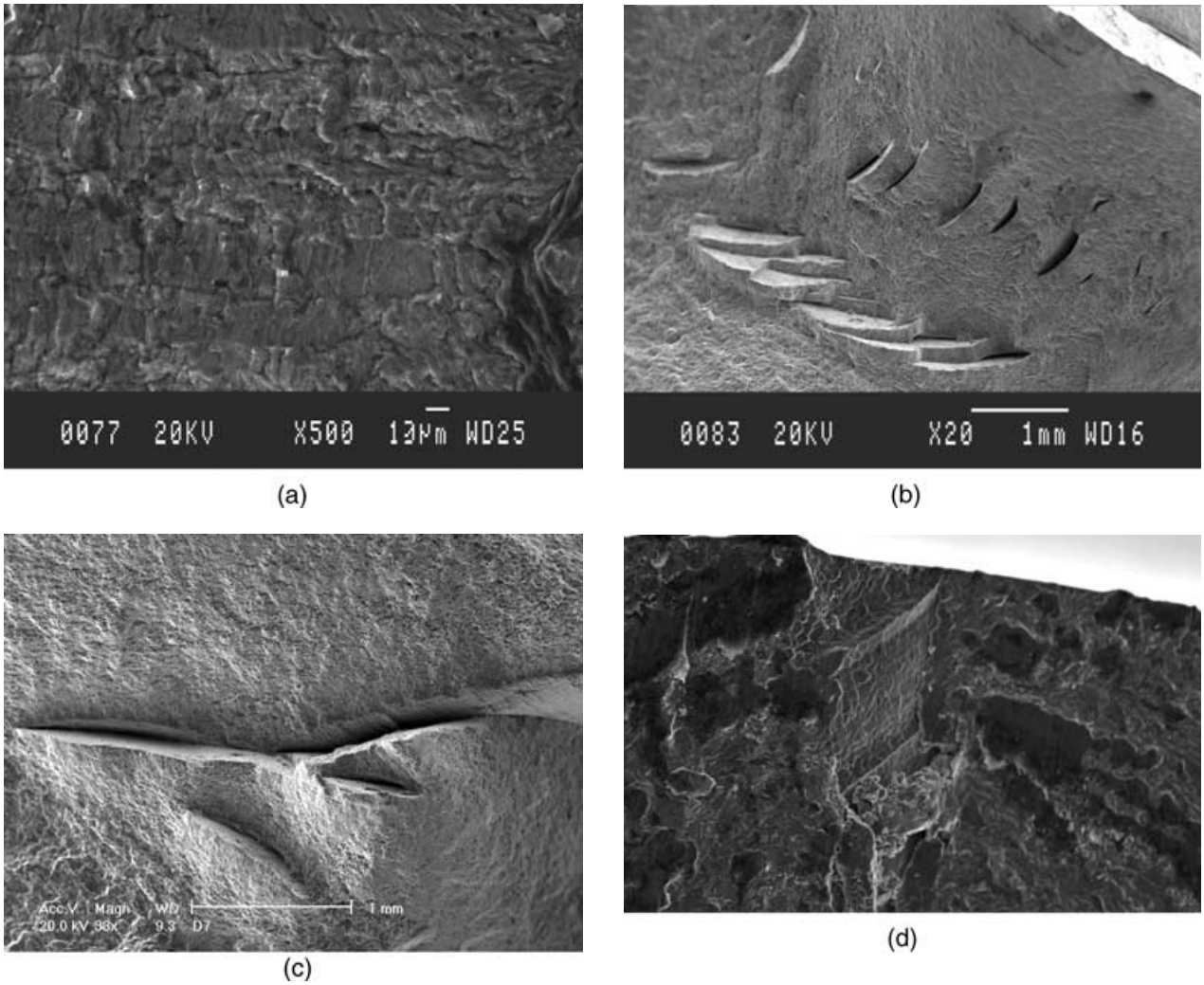

Fig. 9 (a) Banding texture on an FSW fracture surface near the crack-initiation site. (b) Planar facets on the fast fracture region of a bend fatigue specimen. (c) Planar facets on the fast fracture region of a tension specimen. (d) Layer interface linking two small fatigue cracks.

fects can unequivocally be shown to arise in this layered structure, the mechanism behind them is more difficult to identify. Until recently, information on flow processes in FSW has been lacking in the open literature. Thus the large planar fracture surface facets reported by James *et al*.[2] were identified in that paper as 'partial-forging' defects. There may well be some truth in that descriptor, as the pressure and temperature conditions may vary sufficiently in parts of an FS weld to lead to such partial bonds between deposited layers.

However, a recent paper by Guerra *et al*.[8] has provided a description of the formation of the onionskin layers, which provides a framework to explain a number of important observations related to the microstructure in the TMAZ of an FS weld and to their dynamic performance. Reference [8] indicates that the flow of metal during FSW occurs by two main processes. The first involves 'wiping' of material from the advancing front side of the tool onto a zone of metal that rotates and advances with the tool. The material undergoes a helical motion within the rotational zone. After one or more rotations, this zone of metal is sloughed off in the wake of the tool, primarily on the advancing side. The second process is an entrainment of material from the front retreating side of the tool that 'fills in' between the sloughed off pieces. In essence, as proposed by those authors,[8] the metal in the FSW TMAZ consists of two streams of material with different thermo-mechanical histories and mechanical properties. These constitute the layers in the onionskin structure.

This process explains why the layers etch differently, as the different thermo-mechanical histories would lead to different dislocation densities and distributions. It would also be expected that adjacent layers would show different strain-hardening exponents and microhardness

values. This would lead to scatter in microhardness values in the TMAZ and, more importantly, could also lead to strain-partitioning effects occurring during deformation processes. Results on strain measurements during tensile testing, presented by Reynolds at a recent international workshop,[9] clearly indicated that such strain-partitioning did occur between adjacent layers in the TMAZ structure. This effect will be examined by the present authors using strain tomography techniques.

Any propensity towards strain partitioning would be exacerbated by high strain rates during deformation, such as would occur as fatigue crack velocities increase, or under fast fracture. Strain-partitioning mechanisms are often associated with the occurrence of ductility-related cracking problems; two well-known examples are strain-age embrittlement and reheat cracking. It is proposed that the planar defects observed in this work on the fracture surfaces of the specimens represent the operation of a strain-partitioning induced ductility drop at layer interfaces, possibly sometimes coupled with partial forging during welding. Activation of such a mechanism during fatigue or fracture would depend, among other things, on the crack orientation with respect to the interface, the strain rate and the relative differences in mechanical properties and strain hardening exponent of adjacent layers in the onionskin structure.

An effect of orientation of the layers, relative to crack path, can be illustrated by comparing Fig. 4b with Fig. 9a. The latter figure shows banded texture on the fracture surface near the crack initiation site in a tensile fatigue specimen. The width of these bands is around 10–20 μm, much smaller than the tool advance per revolution, and more on a scale with the recrystallised grain size. The details of the structure provide an indication that, if the crack had crossed these layers at a glancing angle, their appearance might then mirror that of the flat region marked A in Fig. 4b. The significance of this structure on dynamic performance is not yet clear.

Figure 9d shows similar fracture surface marks to those seen in Fig. 4b, but here they are directly associated with crack initiation and occurring at an intermediate angle to the surface. This is a particularly interesting example, both because the layer interface defect is acting as a path linking two smaller fatigue cracks near their initiation sites, and because its shape is reminiscent of a threaded helical profile. The sharp protrusions have an apparent spacing of around 0.1 mm. This specimen was tested in reversed bend with $\sigma_{\text{amplitude}} = 130$ MPa, giving a life of 1 204 153 cycles and, as seen in Fig. 7, has a low-fatigue performance.

The occurrence of such defects in FS welds naturally raises the question of how to optimize weld process conditions, so as to minimize defects and maximize dynamic performance. In order to advance in this optimisation, more quantitative information on weld tool forces, torques, energy input and temperature is required. One way of obtaining such insight has been developed by the authors using an instrumented tool, which allows visualisation of the force 'footprint' during welding. Coupled with the use of feedback into computer-controlled welding, initial results indicate significant scope for enhanced understanding of FS welding. The following section introduces the technique and gives some preliminary results obtained with the instrumented tool.

WELD PROCESS CHARACTERIZATION

Improved weld quality and dynamic performance largely rests on achieving a better understanding of the influence of process parameters on tool force and torque footprint during the welding process, and in relating these to defect population and microstructure. This issue is not trivial, as it entails consideration of a number of factors, including tool design, speed, feed, plunge force and rake angle. It should be noted that tool design incorporates pin geometry and ratio of tool shoulder to pin diameter. These parameters are also influential in determining the initial dwell time and the weld length necessary to achieve steady-state process conditions.

To develop an understanding of the process-microstructure-performance characteristics of FSW requires the integration of reliable and accurate sensors into the tool platform, and use of feedback to implement a computerized multivariable control scheme for the weld process. Such an instrumented FSW machine has been used by the authors to provide on-line measurement of the main parameters believed to characterize the FSW process and that hence affect the dynamic fatigue performance of the welds. It measures tool torque, tool temperature, and downwards force applied by the tool shoulder to the material, as well as a horizontal force vector that is measured through 360° as the tool rotates.

The particular relevance of this output to the work in this paper is that of gaining a more sophisticated understanding of the relative effects on the plastic flow processes of tool parameters (shape, feed, speed) as a function of alloy type. These plastic flow processes control the microstructure in the TMAZ[4] and hence will exert a considerable influence on the dynamic performance of an FSW joint. The parameter of most interest is therefore likely to be the horizontal force vector. This can be presented as a polar plot of 'force footprint' that provides process information unique to the tool geometry, alloy and weld pitch (tool increment per revolution).

As defined in this paper, the force footprint is a graphical representation of the resultant force vector experienced by the tool during a single revolution, which can therefore be resolved to give the X and Y forces at any angle. The area contained within the polar plot is then a measure of

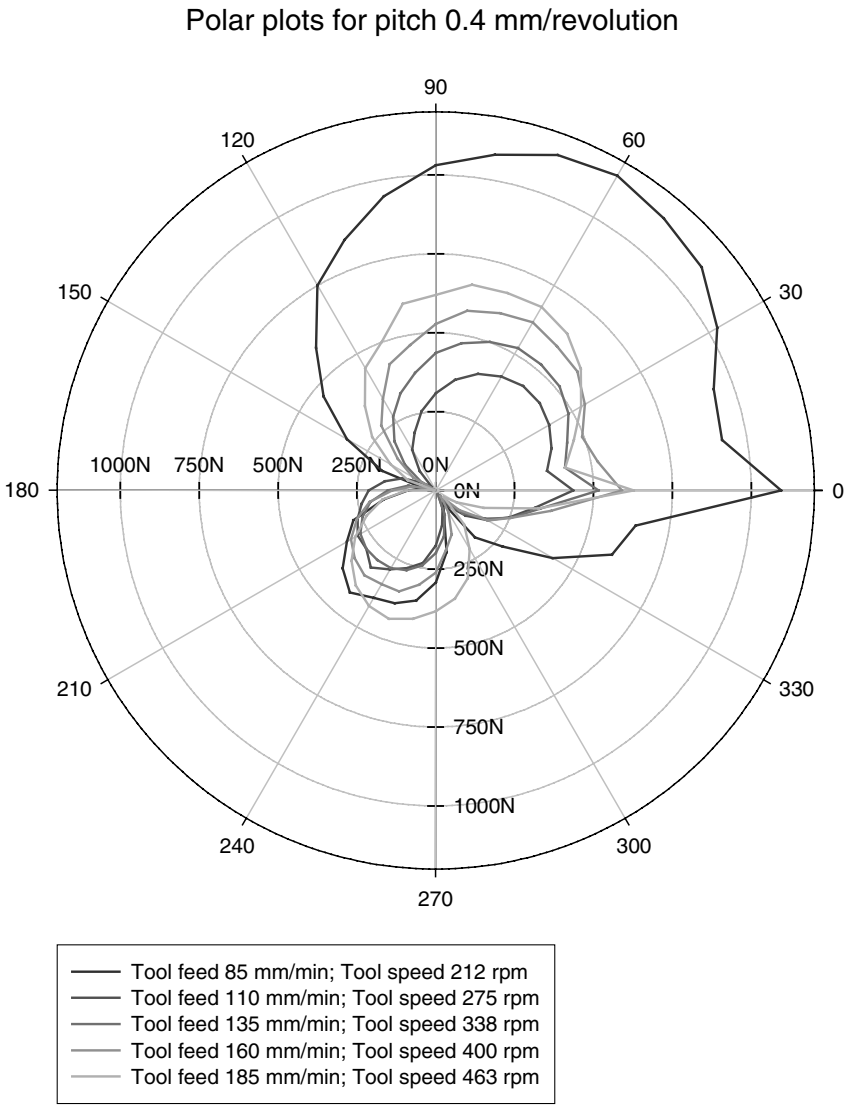

Fig. 10 Polar plot force footprint diagrams showing the effect of changing tool feed and speed, for a constant value of weld pitch = 0.4 mm per revolution.

the rotational energy input into the weld, which should be capable of correlation with the plastic flow processes in the weld, the defect population and hence the dynamic performance. Thus weld soundness and performance should be capable of explicit linking with process conditions (e.g. tool pitch, which is defined as weld travel increment per revolution) as a function of alloy and tool design.

Figure 10 shows a set of polar force footprint diagrams obtained for FSW welds in 5083-H321 alloy with a constant value of weld pitch of 0.4 mm per revolution. As tool feed and speed vary, so the area inside the polar plot diagrams varies in a systematic way. It is possible to obtain a series of such plots at different values of weld pitch and to determine the area contained within the force locus. This area is related to the energy input by the tool into the weld, and should therefore be linked to weld properties and performance. The data can be presented as a contour map of nominal energy input into the weld as a function of several different parameters. Figure 11 shows such a plot as a function of weld pitch and tool speed.

It is clear that this type of presentation of weld-process information will throw valuable light on useful avenues of exploration for FSW process optimization. These maps should also be capable of being related to the presence of defects, and to variations in mechanical property values and fatigue performance. The net result of such research efforts is likely to be a substantial improvement in the ability to predict appropriate welding conditions for

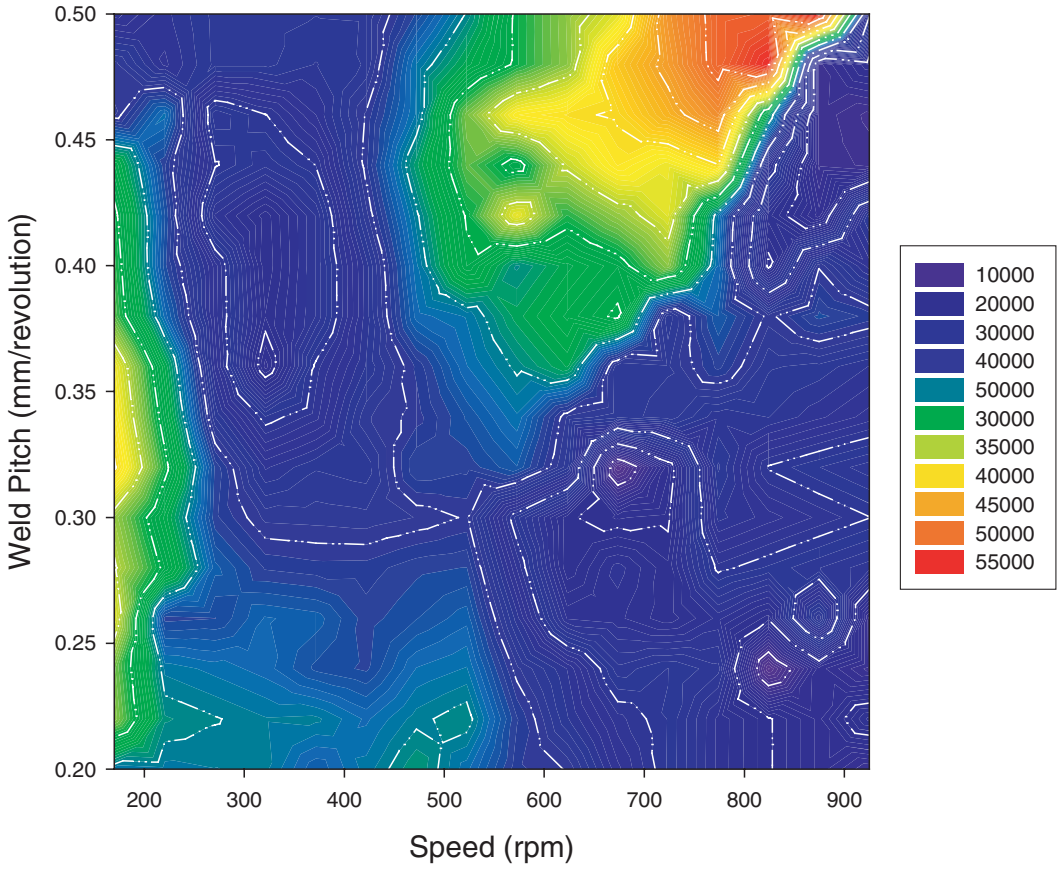

Fig. 11 Contour plot of polar plot area (which is related to energy input) as a function of weld pitch and tool speed.

various combinations of alloy, plate thickness, tool design and production rates.

CONCLUSIONS

This paper has presented some observations and discussion centred around the interaction between the dynamics of the FS welding process, its influence on crack path defects and their significance for fatigue and fracture performance. In particular, an explanation for the origins of planar facets on the fracture surface and their effect on fatigue life has been proposed. This explanation draws on the work of other research groups[8,9] regarding the plastic flow processes that occur during FSW and the strain-partitioning during loading that occurs in adjacent layers of the TMAZ that have different thermo-mechanical histories. The paper has then presented initial results for polar force footprint diagrams obtained using an instrumented FSW machine. These plots can be analysed to obtain information relevant to process optimisation, to defect populations, mechanical properties and dynamic fatigue performance.

The main conclusions can be summarized as follows:

- Planar facets occur on the fracture surfaces of FSW welds in 5×83-H321 aluminium alloy with sizes in a range from 0.1 to 1.5 mm.
- These facets are believed to arise from an interface ductility drop induced by strain partitioning that occurs in adjacent layers in the TMAZ during loading. Their occurrence is enhanced by higher strain rates, but they also occur near crack-initiation sites.
- These interfacial strain-partitioning defects can reduce fatigue strength of FSW specimens by up to 20%.
- The study of crack path subtleties through fractography forms an indispensable part of the overall analysis of fatigue crack paths.
- Instrumented FS welding allows the determination of polar force diagrams which can shed light on the relationship among process parameters, microstructure and fatigue performance.
- Analysis of the force footprint relationships seems likely to lead to optimization of the FSW process, and to a reduction in the empiricism associated with choice of

welding-process conditions. In turn, this should allow the consistent fabrication of welds with higher levels of fatigue performance.

Acknowledgements

The assistance of T.C. Yio with some of the experimental work and the support of Corus Research & Development, Rotherham in funding the FS welding is gratefully acknowledged.

REFERENCES

1 Pook, L. P. (2002) *Crack Paths*. WIT Press, Southampton.
2 James, M. N., Hattingh, D. G. and Bradley, G. R. (2003) Weld tool travel speed effects on fatigue life of friction stir welds in 5083 aluminium. *Int. J. Fatigue* **25**, 1389–1398.
3 Lamarre, A. and Moles, M. (2000) Ultrasound phased array inspection technology for the evaluation of friction stir welds. In: *Proceedings of 15th World Conference on Nondestructive Testing*. Rome, Italy, October 2000. Available at http://www.ndt.net/article/wcndt00/index.htm.
4 Bendzsak, G. J., North, T. H. and Smith, C. B. (2000) An experimentally validated 3D model for friction stir welding. In: *Proceedings of the 2nd Friction Stir Welding Symp*. Gothenburg, Sweden, June 2000, TWI, Cambridge.
5 Lienert, T. J., Stellwag, W. L., Grimmett, B. B. and Warke R.W. (2003) Friction stir welding studies on mild steel. *Welding J.*, 1S–9S.
6 Dickerson, T. L. and Przydatek, J. (2003) Fatigue of friction stir welds in aluminium alloys that contain root flaws. *Int. J. Fatigue* **25**, 1399–1409.
7 Dalle Donne, C., Biallas, G., Ghidini, T., *et al*. (2000) Effect of weld imperfections and residual stresses on the fatigue crack propagation in friction stir welded joints. In: *Proceedings of 2nd Friction Stir Welding Symposium*. Gothenburg, Sweden, June 2000, TWI, Cambridge.
8 Guerra, M., Schmidt, C., McClure, J.C., *et al*. (2003) Flow patterns during friction stir welding. *Mats. Charact.* **49**, 95–101.
9 Reynolds, A. P. (2003) Presentation at *International Workshop on FSW*, Port Elizabeth Technikon, April 2003.